Electronic Supplementary Material (ESI) for Nanoscale.

Interfacial tension driven adsorption of MnO_2 nanoparticles at the liquid/liquid interface to tailor ultra-thin polypyrrole sheets

Subin Kaladi Chondath[†], *Abhishek Pradeep Kumar Sreekala*[†], *Chalikkara Farzeena*[ǂ], *Subramanyan Namboodiri Varanakkottu*[ξ], *Mini Mol Menamparambath*[†,*]

[†]Department of Chemistry, National Institute of Technology Calicut, Calicut-673601, Kerala, India.

[ǂ]School of Materials Science and Engineering, National Institute of Technology Calicut, Calicut-673601, Kerala, India.

[ξ]Department of Physics, National Institute of Technology Calicut, Calicut-673601, Kerala, India.

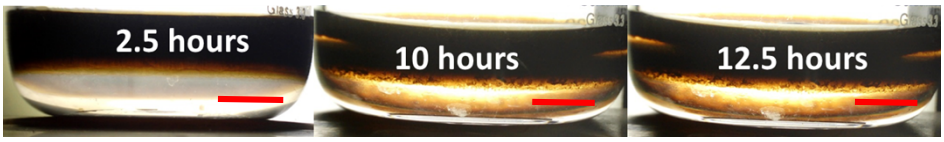

Fig. S1. Photographic images of PPy/MnO_2 synthesized at bisolvent system after 2.5, 10, and 12.5 hours. The evident product confinement at the interface starts at 10 hours. Scale bar: 1 cm.

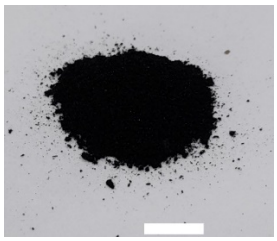

Fig. S2. Photographic image of PPy/MnO_2 sheets in their powder form obtained after purification followed by room temperature vacuum drying for 24 hours. Scale bar: 0.5 cm.

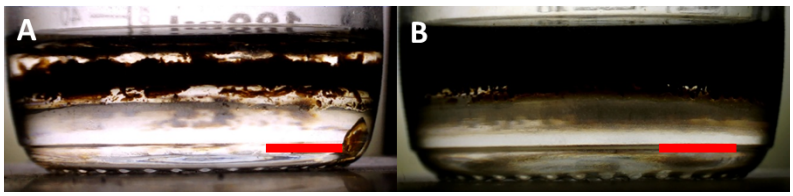

Fig. S3 Photographic images of PPy/MnO_2 synthesized using water/chloroform interface at a monomer and oxidant concentration of (A) 0.005 M and (B) 0.02 M, respectively in chloroform and water. Scale bar: 1 cm.

The PPy/MnO_2 formed in Fig. S3 A showed product confinement at the water/chloroform interface. The products in Fig. S3 B were found to be dispersed at the polar aqueous phase. The formation of a

stable aqueous dispersion of products (Fig. S3 B) is due to the over-oxidation, and secondary growth of NP-attached oligomers during the polymerization. The polymerization is initiated by the redox reaction between the monomer and oxidant at the interface leading to the subsequent formation of MnO_2 attached oligomers. Unlike 0.005 M and 0.01 M concentrations, the interfacial tension is insufficient to confine the excess concentration of MnO_2 attached oligomers at the interface. Hence, MnO_2 attached oligomers are highly unstable at the interface and migrate to the polar aqueous phase, resulting in over-oxidation and secondary growth under the influence of a higher amount of oxidants.

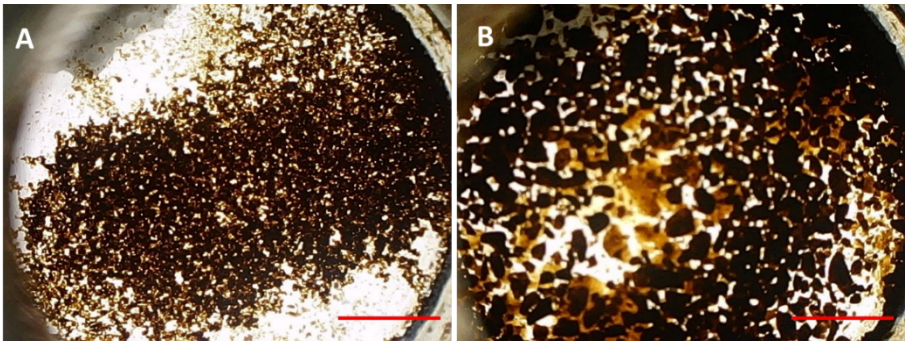

Fig. S4 Top-view photographic images of PPy/MnO_2 synthesized using water/chloroform interface at a monomer and oxidant concentration of (A) 0.005 M and (B) 0.01 M, respectively, in chloroform and water. Scale bar: 1 cm. The reaction at 0.01 M concentration showed more interfacial product confinement than 0.005 M.

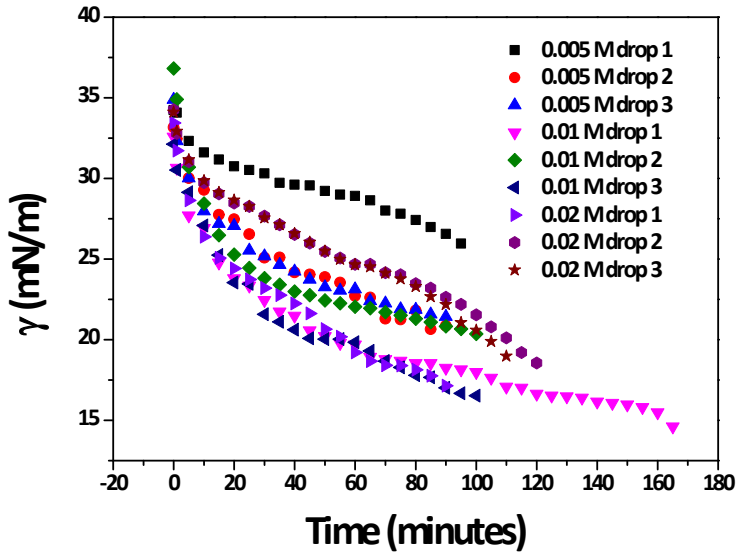

Fig. S5 Dynamic interfacial tension measured as a function of reaction time for bisolvent systems corresponding to three drops (drops 1, 2, and 3) of different monomer/oxidant concentrations (0.005 M, 0.01 M, and 0.02 M).

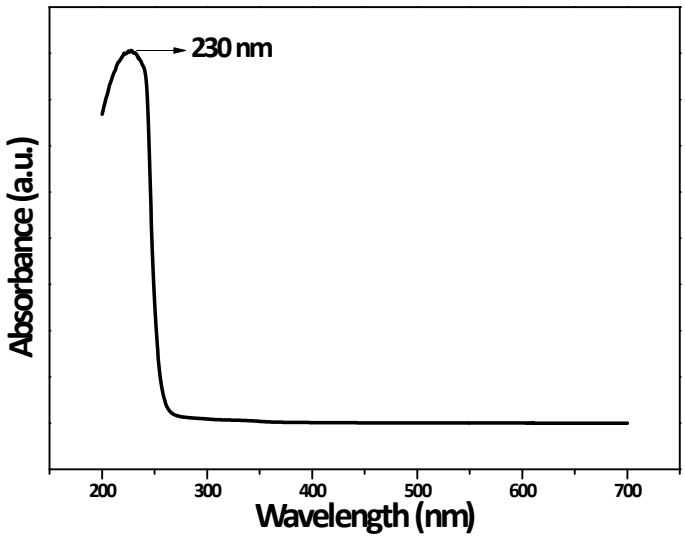

Fig. S6 The UV-Vis absorption spectrum of pyrrole monomer dispersed in water.

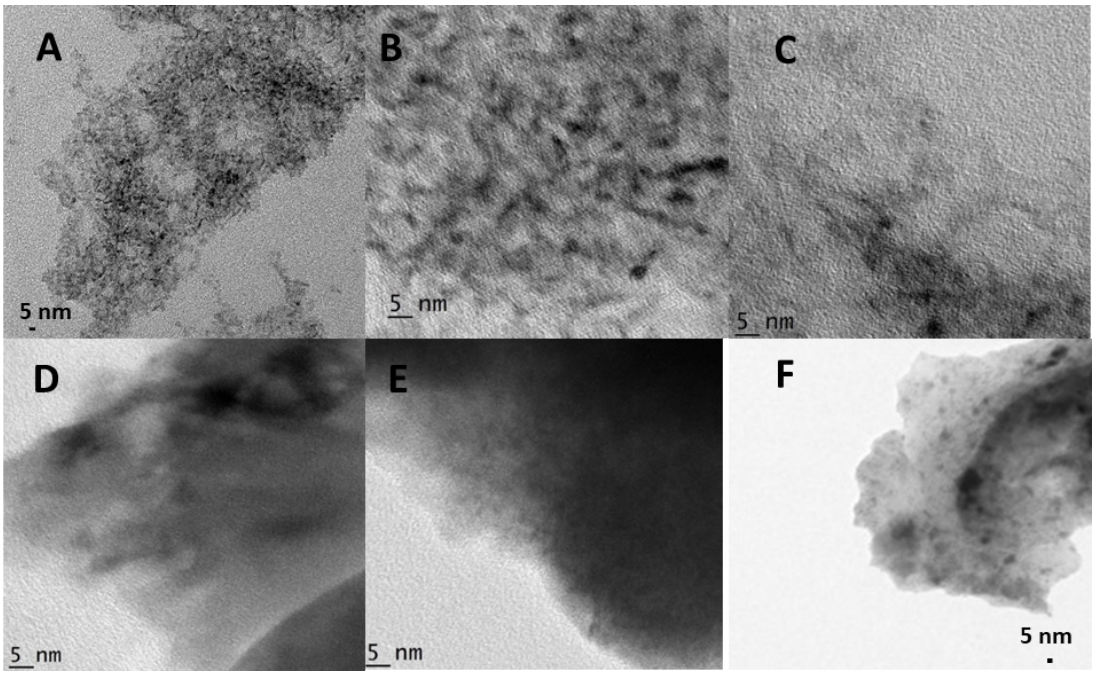

Fig. S7 High magnification TEM images of PPy/MnO_2 separated from the bisolvent medium at different time intervals. (A) 2.5 hours, (B) 5 hours, (C) 7.5 hours, (D) 10 hours, (E) 12.5 hours, and (F) 15 hours.

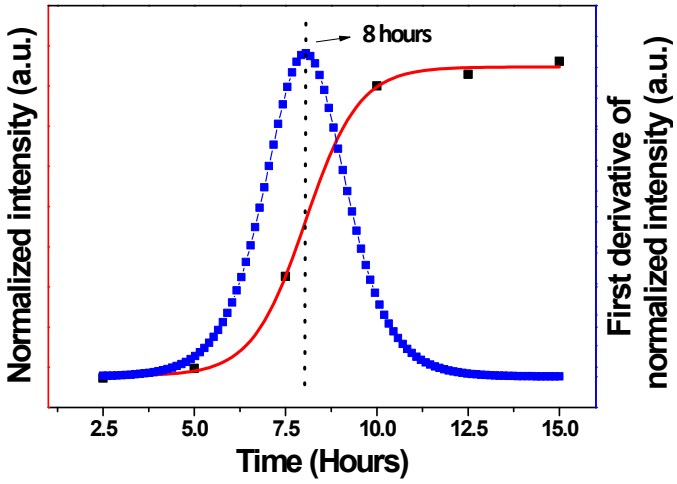

Fig. S8 The normalized intensity of (310) plane from the SAED patterns of PPy/MnO_2 and its first derivative plotted against reaction time.

The PPy/MnO_2 synthesized in 2.5 – 7.5 hours showed less intense Bragg spots or rings as compared to the samples prepared in 10-15 hours. This may be due to the distinguishable transition of morphology from agglomerated networks (2.5, 5, and 7.5 hours) to 2-D sheets (10, 12.5, and 15 hours) with the encapsulation of crystalline MnO_2 NPs.

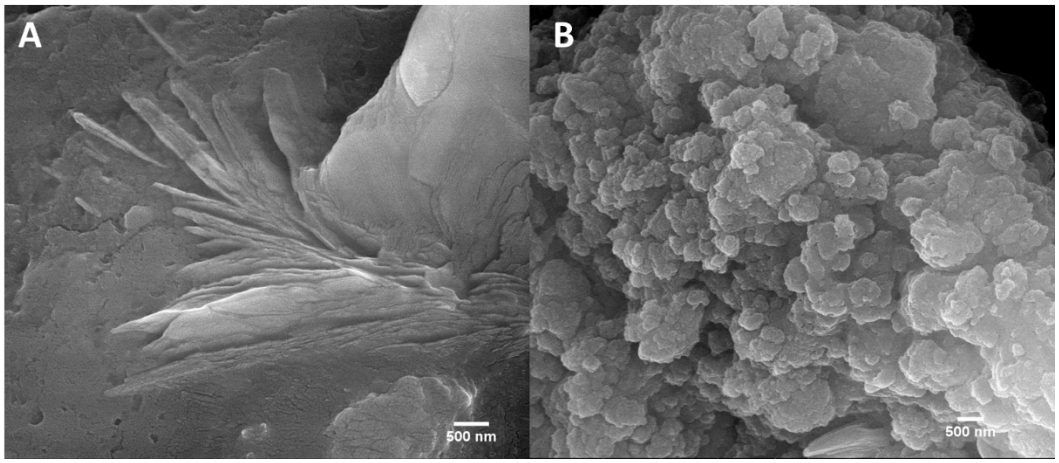

Fig. S9 The FESEM images of PPy/MnO_2 synthesized at (A) water/chloroform interface and (B) aqueous medium. The reaction time was 15 hours.

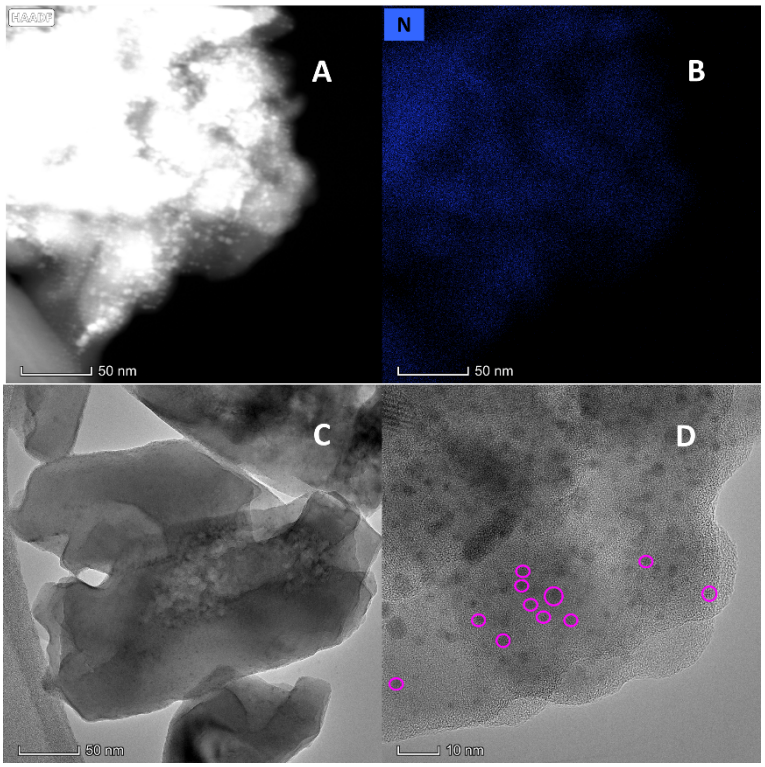

Fig. S10 (A) HRTEM image of PPy/MnO_2 sheets. (B) Elemental mapping image of nitrogen in PPy/MnO_2 sheets. (C) High-resolution TEM image of PPy/MnO_2 sheets showing a few-layer nature of PPy sheets with embedded MnO_2 NPs. (D) The dark spots in the images represent (pink circles) uniformly embedded MnO_2 NPs, and the lighter grey portions represent PPy sheets.

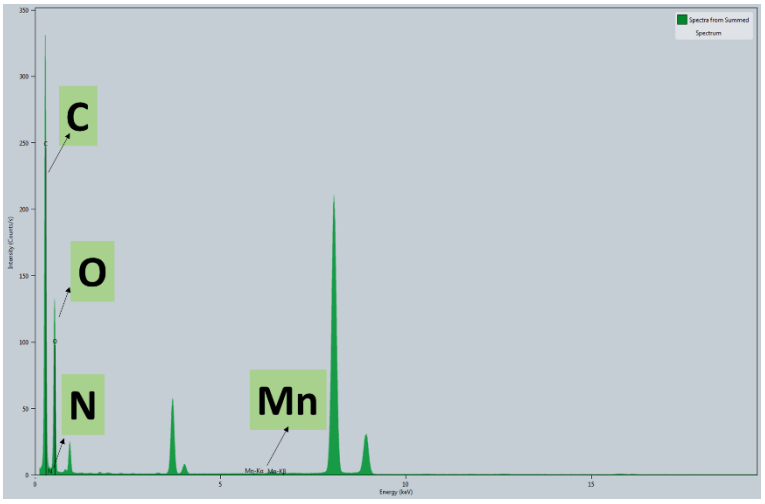

Fig. S11 HRTEM-EDS spectrum of PPy/MnO_2 sheets.

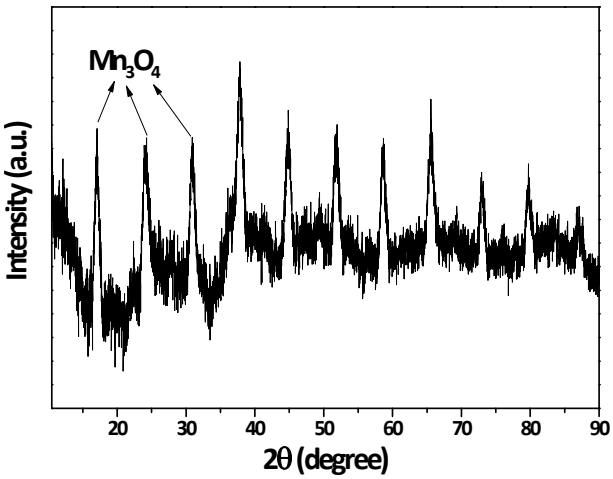

Fig S12. XRD spectrum of PPy/MnO_2 synthesized in the single solvent system.

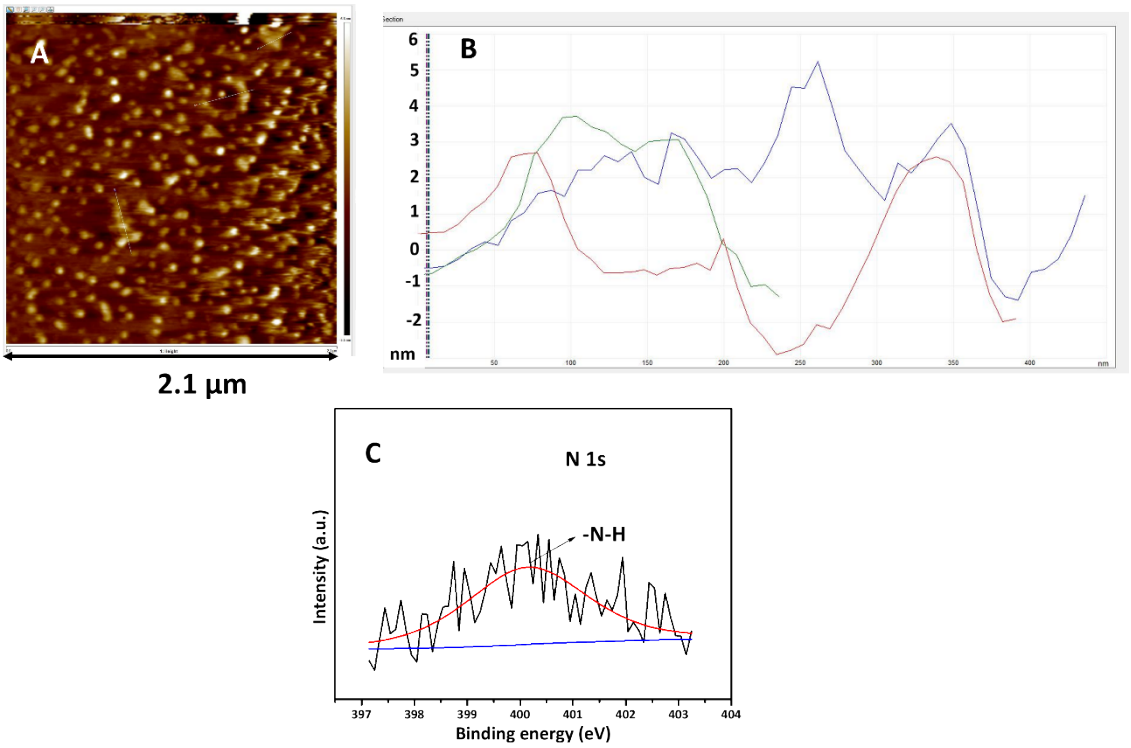

Fig S13. (A) 2-D surface AFM image and (B) surface profile recorded from three different scans. (C) High-resolution N 1s spectrum

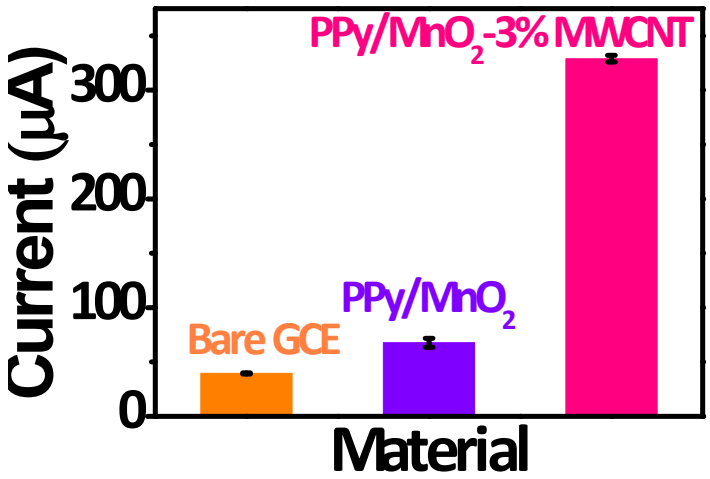

Fig. S14 Maximum anodic current in the cyclic voltammetric responses of 1 mM nicotine on various modified electrodes.

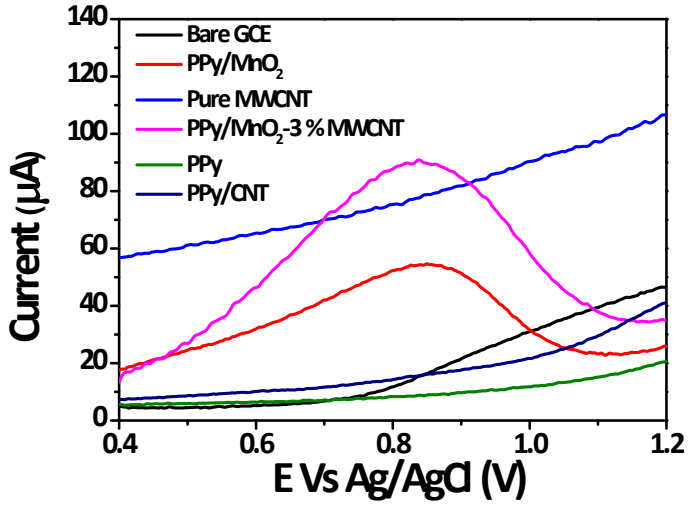

Fig. S15 Differential pulse voltammetry responses of 1 mM nicotine on various modified electrodes.

The DPV scans show apparent oxidation peaks for PPy/MnO_2 and PPy/MnO_2-3% MWCNT. PPy/MnO_2 offers a maximum current of 54 μA at 0.84 V, whereas PPy/MnO_2-3% MWCNT furnishes nicotine oxidation at a high current of 92 μA at 0.93 V.

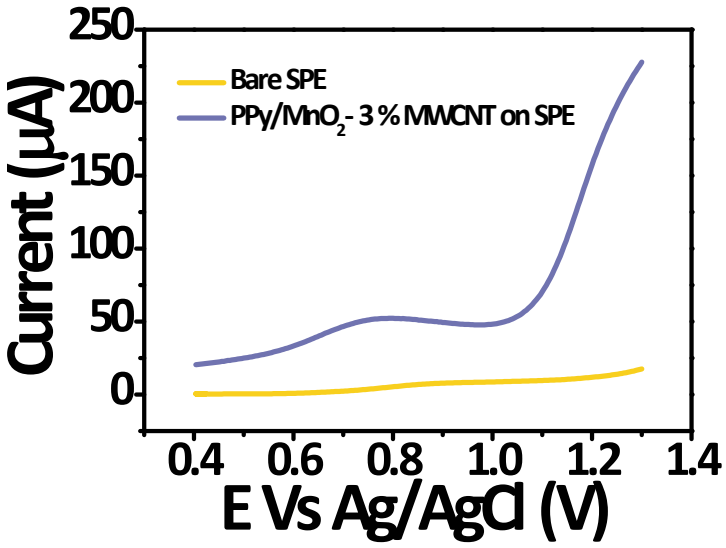

Fig. S16 Differential pulse voltammetry responses of 1 mM nicotine on bare SPE and modified SPE. The PPy/MnO_2 – 3 % MWCNT modified SPE offers a maximum current of 55 µA at 0.79 V.